Thanks to the referee for his/her very thoughtful suggestions. Below we address the reviewers' comments, with the reviewer comments in black, and our response in blue. We have revised the manuscript accordingly, and mentioned the line number of the **tracked revision**.

Anonymous Referee #2:

General comments:

East Asian countries and regions are always suffered from serious air pollutions with rapid economic growth in recent decades. And high level emissions of air pollutants in East Asia could further affect regional air qualities, human health, traffic safeties as well as regional or global climate changes. Observations have revealed that severe and persistent haze pollutions occurred frequently in China during recent years. Although the numerical models could capture the loading levels and temporal-spatial variations of the total PM, most of them could not well simulate their chemical components, especially in heavy pollution episodes. Thus, accurately predicting the concentrations and chemical components of particulate matter are still very challenging for climate and air quality models. In this study, influence of aqueous-phase chemistry on the formation of near surface sulfate as well as the concentrations of total ammonium is carried out to investigate the importance of this process in some polluted episodes, based on observations and numerical evolutions. Therefore, the topic of this study is interesting and novel to some degrees and the paper has a potential for publication in the journal.

Thanks to the reviewer for the comments and suggestions.

Specific Comments:

1. Both Abstract and Conclusions should be more concise, instead of only repeating the results.

We have revised the Abstract and Conclusions.

2. Were the aerosol or trace gases from biomass burning taken into account in the simulations? What is the resolution of the emission inventory (MEIC)? Why the emissions in 2016 were used to assess the pollution episode in 2018?

According to previous studies (Du et al., 2017; Wu et al., 2018), the peak emissions of biomass burning are normally found in summer and autumn harvest periods, including May, June, September, and October, while the contribution of biomass burning emission to the pollutants in winter is generally low. From the MODIS Fire and Thermal Anomalies product, the detective hotspots are sparse during this haze-fog event in the YRD, thus the contribution of biomass burning emission is deemed to be minimal in this study case (Fig. R1). Therefore, the aerosols and trace gases from biomass burning are not considered in the simulations.

To quantify the impact of biomass burning emission on aerosols and trace gases concentrations, we conducted an additional simulation with biomass burning emission

(i.e., BBE). The biomass burning emission is taken from Fire INventory from NCAR (FINN), including the emissions of CO_2, CO, NO, NO_2, SO_2, NH_3, OC, BC, PM, CH_4, and NMVOC, etc. From Fig. R2, the emissions of SO_2, NO_x, and NH_3 from biomass burning are distributed sporadically in the YRD, with the total emissions less than 219 kg km^{-2} for SO_2, 254 N kg km^{-2} for NO_x, 491 kg km^{-2} for NH_3 during this period. The contribution of biomass burning to total SO_2, NO_2, and NH_3 emissions is zero in most areas. Only in some small places, biomass burning accounts for half of the total emissions. Additionally, we quantify the impacts of biomass burning emission on the simulated SO_2, NO_2, NH_3, and $PM_{2.5}$ (Fig. R3). Biomass burning emissions only change the mean concentrations of air pollutants (SO_2, NO_2, NH_3, SNA, and $PM_{2.5}$) by less than 10% during this period in the YRD. Therefore, biomass burning emissions have little impact on air pollutants concentrations during this period, and we do not need to consider biomass burning emissions in this study.

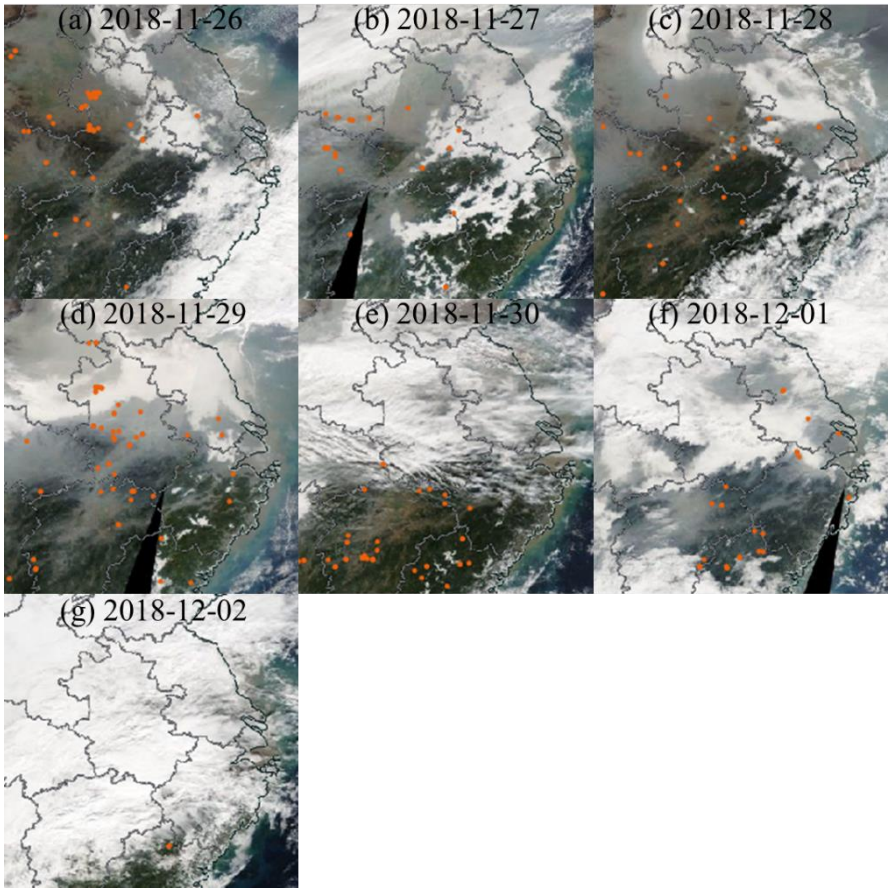

Figure R1. MODIS hotspots from 26 November to 2 December in the YRD.

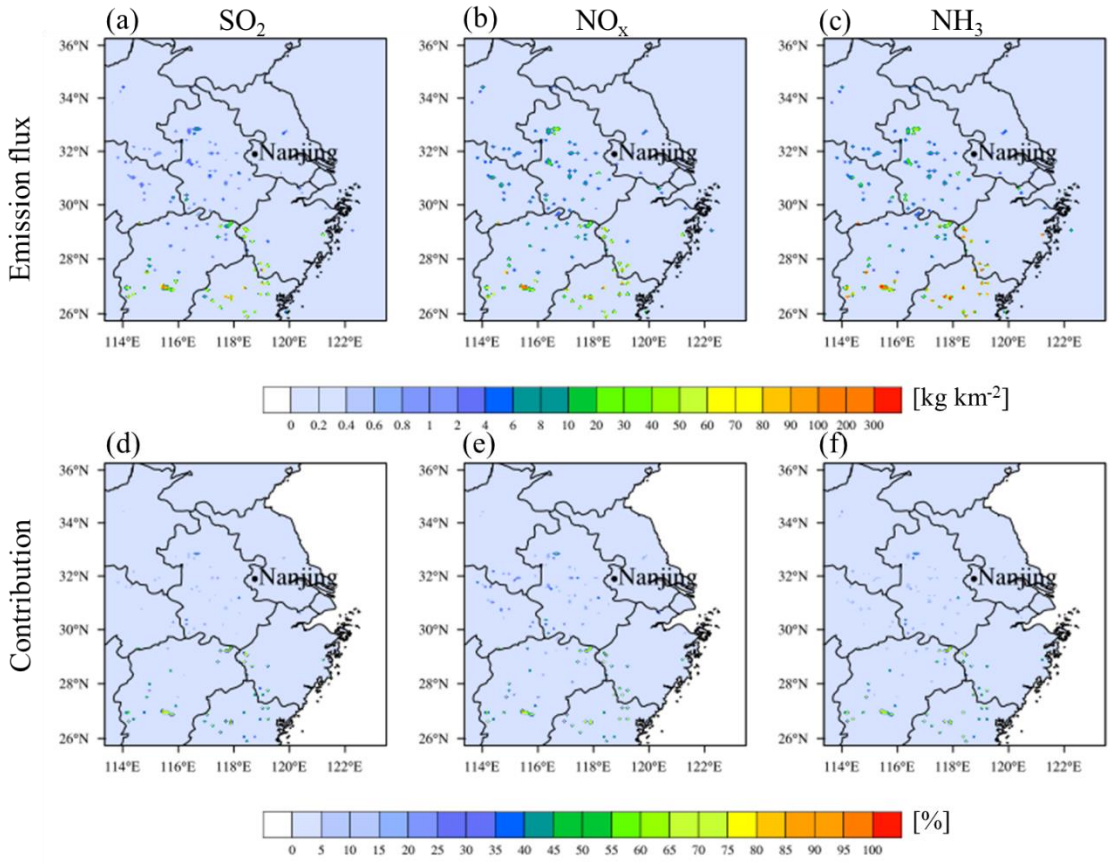

Figure R2. Spatial distribution of total biomass burning emission for (a) SO_2, (b) NO_x, and (c) NH_3 (unit: kg km^{-2}), as well as the contribution of biomass burning to total emissions for (d) SO_2, (e) NO_x and (f) NH_3 during the haze-fog event in the YRD.

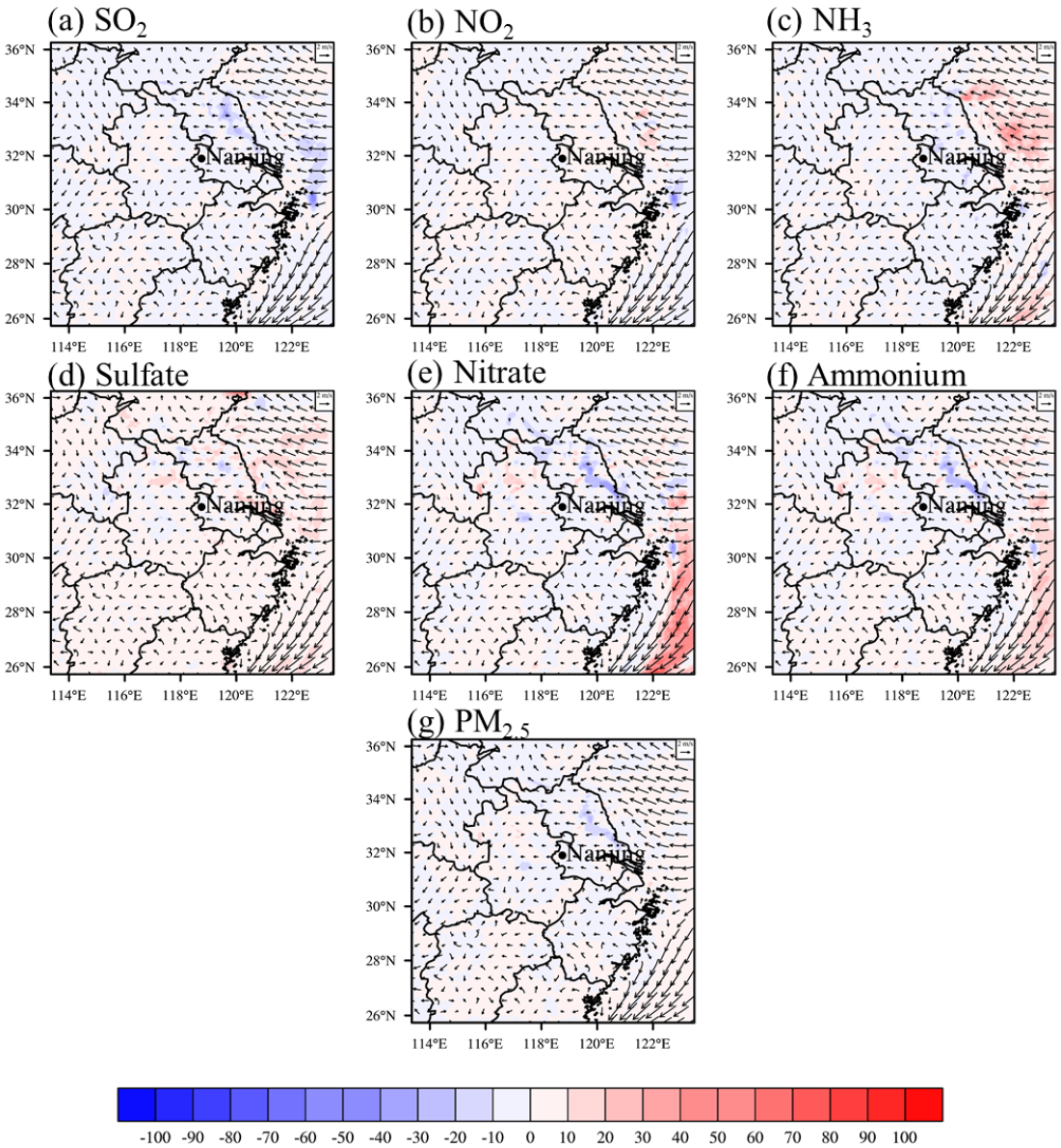

Figure R3. The impacts of biomass burning emissions on simulated (a) SO_2, (b) NO_2, (c) NH_3, (d) sulfate, (e) nitrate, (f) ammonium, and (g) $PM_{2.5}$ concentrations during the haze-fog event in the YRD, calculated as the difference between the Control and BBE simulations.

The resolution of MEIC emission inventory is 0.25°×0.25°. We have added the details in the revised version, see line 198.

The latest anthropogenic emission inventory available when we were doing this study was MEIC 2016.

3. What is the resolution of the Himawari-8 and MODIS data? Is the MODIS resolution accurate enough to evaluate the model?

The Advanced Himawari Imager (AHI) data from the Himawari-8 satellite has 16 channels with central wavelengths ranging from 0.47 μm to 13.3 μm. The spatial

resolution of the AHI pixel is 0.5 km for band 3; 1 km for bands 1, 2, and 4; and 2 km for the other bands. Three visible bands, i.e., red (band 3, 0.64 μm), green (band 2, 0.51 μm), and blue (band 1, 0.47 μm) are used to show the fog area. The resolution of the MODIS satellite data is 1°. We have added the details in the revised version, see lines 238-242, and 244-245.

We compared the spatial distribution of observed LWP from MODIS Collection L3 (MYD08) and L2 (MYD06) cloud products. The resolution of MODIS L2 LWP is 1×1 km^2 (nadir) and was re-gridded to the model grid (9×9 km^2). Fig. R4 shows that the distribution of LWP from MODIS L2 product is similar to the L3 product during the haze-fog event in the YRD, except on 27 and 30 November, which the location of high LWP in the two products is slightly different. We also compared the cumulative probability distribution of LWP from MODIS L3 and L2 products (Fig. R5). The cumulative probability distribution of LWP from MODIS L2 is similar to the L3. The constraining equation for transforming the modelled LWP with using the MODIS L2 LWP is:

$$x_{\mathrm{m}}^{\mathrm{c}} = 61.0 \times (x_{\mathrm{m}} + 5.8)^{0.33} + 1.9 \quad (1)$$

Which has a similar constrained function as using the MODIS L3 product (i.e., $x_{\mathrm{m}}^{\mathrm{c}} = 53.0 \times (x_{\mathrm{m}} + 5.8)^{0.4} - 1$). Therefore, LWP from the MODIS L3 product is accurate to evaluate the model and constrain the simulated LWP, and we do not expect an influence of the MODIS resolution on the results herein.

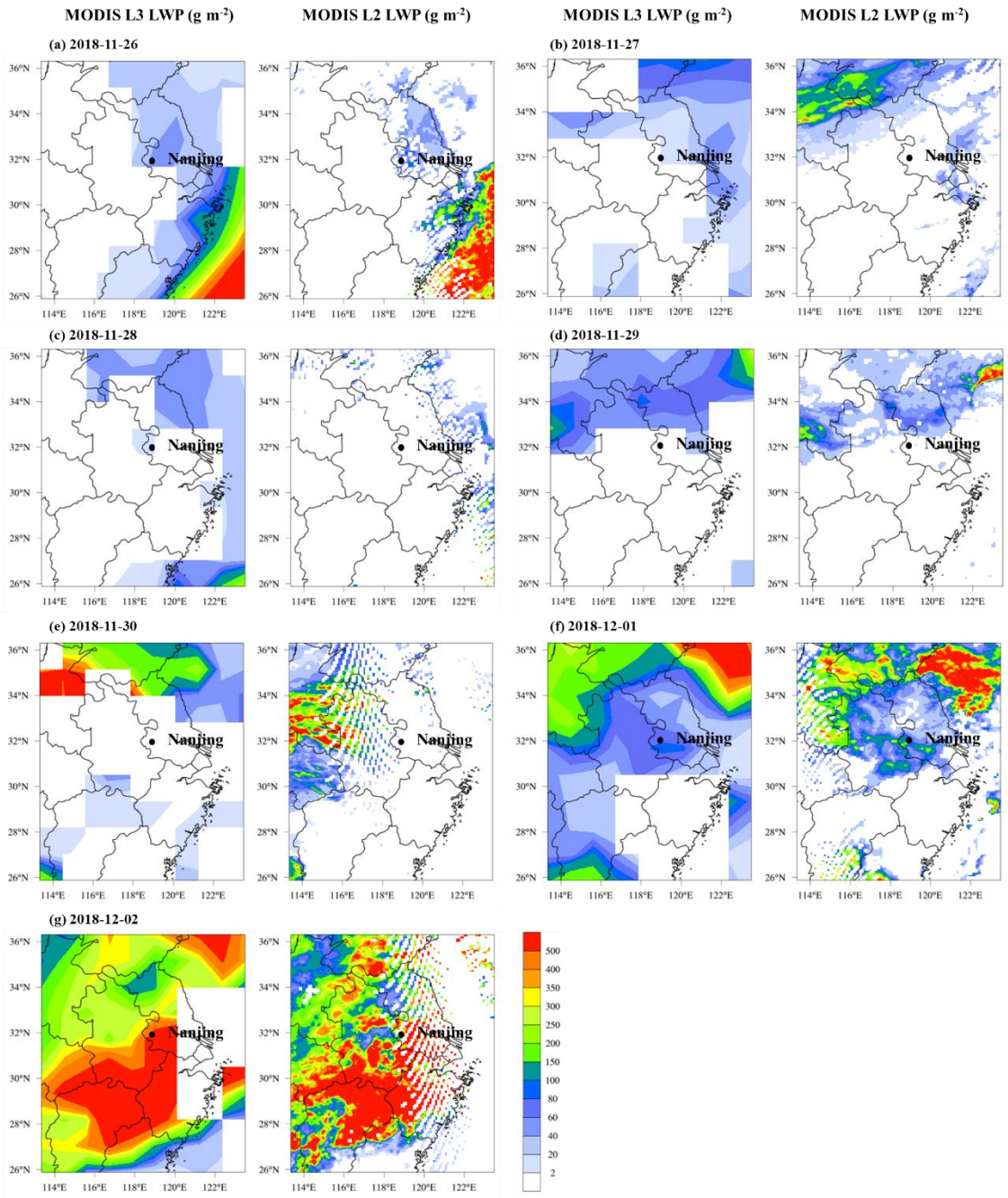

Figure R4. Distribution of the observed LWP (unit: g m^{-2}) from the MODIS Collection 6 Level-3 (columns 1 and 3) and Level-2 cloud product (columns 2 and 4) at 13:30 LT from 26 November to 2 December in the YRD.

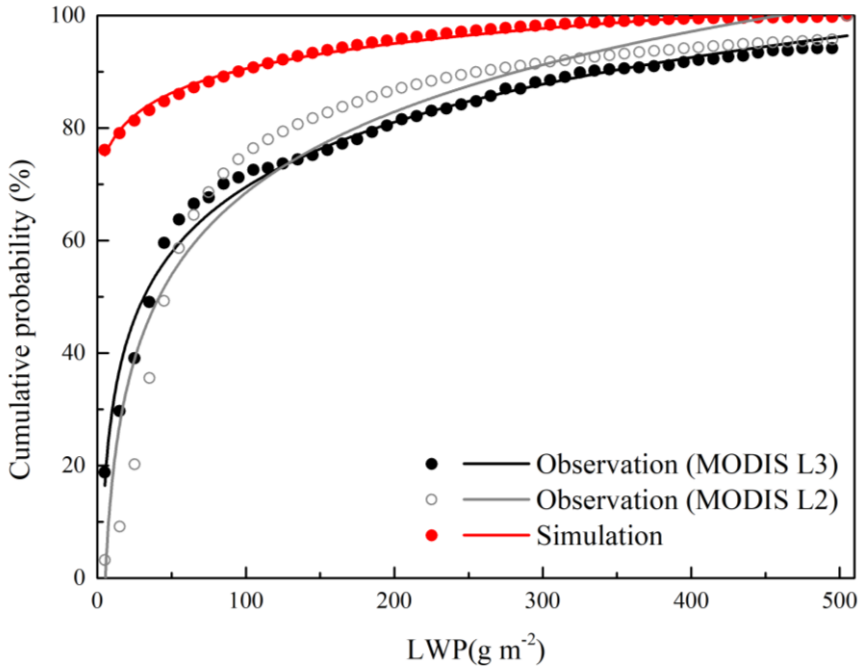

Figure R5. The cumulative probability distribution of LWP from the MODIS observations (L2 and L3 cloud product) and Control simulation (shown as circles). Results are based on statistics of the observed and simulated daily LWP during the haze-fog event in the YRD. The lines present the fitting functions.

4. It seems that the simulated ammonium (NH4+) has little improvement when simulated the corrected LWC is used. Why?

This could be ascribed to the underestimation of aerosol water pH in the model. The hydrogen ion activity in aqueous aerosols can affect the partitioning of TNO_3 and TNH_4 between the gas and aerosol phase. Lower aerosol water pH favors partitioning of TNO_3 toward gaseous HNO_3 rather than aerosol nitrate. In contrast, TNH_4 partitions toward gaseous NH_3 at higher aerosol water pH (Weber et al., 2016). The simulated $PM_{2.5}$ pH in Sen_c_pH is lower than the observations (Fig. S6), which is conducive to the existence of aerosol ammonium.

We have added the explanations in the revised version, see lines 493-503.

5. Was the VIS calculated based on the aerosol and trace gases in the model? If so, then the overestimated VIS in the model could not be used to illustrate the reason why simulated LWC is underestimated.

The function of visibility (VIS) (Gultepe et al., 2006) is as follows:

$$\mathrm{VIS[m]} = 1002/(\mathrm{LWC[g\,cm^{-3}]} \times \mathrm{N_c[cm^{-3}]})^{0.6473}$$

which is only dependent on LWC and cloud droplet number (N_c).

6. Results in this study states that aqueous-phase chemistry plays a very important role in resulting in severe haze pollution. However, there have many polluted episodes in

which inorganic aerosols are also growth sharply in the absent of fogs. The authors should make a brief comparison or statement on these two types of pollutions in Results.
We agree with the reviewer that the formation of inorganic aerosols can be promoted through aqueous-phase chemistry in cloud/fog water, and inorganic aerosols can be released when the fog dissipates, leading to an increase in aerosol concentrations, especially for sulfate since in-cloud aqueous-phase chemistry can contribute a large fraction to the sulfate production.

According to the observed RH2 and VIS in Nanjing, we divide the haze-fog event into two stages, the formation and development of fog (RH2 $\geq$ 90% and VIS $\leq$ 1 km), and the dissipation of fog (RH2 < 90% and VIS > 1 km) (Fig. S5) (Liu et al., 2018). The observed sulfate, nitrate, ammonium, and $PM_{2.5}$ concentrations all increase when fog dissipates, which are 23%, 24%, 14%, and 17% higher than the concentrations in the formation and development of fog. These results are similar to Zou et al. (2020), indicating that the wet deposition effect of fog on aerosol is negligible if the fog cannot form precipitation, and the aerosols can return to the atmosphere from the fog droplets when the fog dissipates, i.e., fog facilitates the increase of inorganic aerosol concentrations by aqueous-phase chemistry and plays an important role in the occurrence of haze event in moist areas.

We have added the above discussions in the revised version, see lines 297-307.

7. Fig. 6 is needed to be re-plotted. The circles in the figure could be drawn in larger sizes.
Thanks for suggestions, we have re-plotted it.

8. English should be corrected throughout the whole manuscript.
Thanks for suggestions, we have corrected the writing throughout the whole manuscript.

Reference:

Du, W., Zhang, Y., Chen, Y., Xu, L., Chen, J., Deng, J., Hong, Y., and Xiao, H.: Chemical Characterization and Source Apportionment of PM2.5 during Spring and Winter in the Yangtze River Delta, China, Aerosol Air Qual. Res., 17: 2165-2180, https://doi.org/10.4209/aaqr.2017.03.0108, 2017.

Gultepe, I., Müller, M. D., and Boybeyi, Z.: A New Visibility Parameterization for Warm-Fog Applications in Numerical Weather Prediction Models, J. Appl. Meteorol. Climatol., 45, 1469–1480, https://doi.org/10.1175/jam2423.1, 2006.

Liu, W. J., Han, Y. X., Li, J. X., Tian, X. R., and Liu, Y. G.: Factors affecting relative humidity and its relationship with the long-term variation of fog-haze events in the Yangtze River Delta, Atmos. Environ., 193, 242e250, https://doi.org/10.1016/j.atmosenv.2018.0, 2018.

Weber, R. J., Guo, H., Russell, A. G., and Nenes, A.: High aerosol acidity despite declining atmospheric sulfate concentrations over the past 15 years, Nat. Geosci., 9, 282–285, https://doi.org/10.1038/ngeo2665, 2016.

Wu, J., Kong, S., Wu, F., Cheng, Y., Zheng, S., Yan, Q., Zheng, H., Yang, G., Zheng, M., Liu, D., Zhao, D., and Qi, S.: Estimating the open biomass burning emissions in central and eastern China from 2003 to 2015 based on satellite observation, Atmos. Chem. Phys., 18, 11623–11646, https://doi.org/10.5194/acp-18-11623-2018, 2018.

Zou, J., Sun, J., Li, T., Han, X., Xiang, Z. and Sha, J.: Observed Interactions Among Haze, Fog and Atmospheric Boundary Layer during a Haze-fog Episode in the Yangtze River Delta Region, Eastern China, Aerosol Air Qual. Res., https://doi.org/10.4209/aaqr.2020.06.0354, 2020.